Mem. S.A.It. Vol. 84, 707

Memorie della

Model-independent decomposition of broad-band Suzaku spectra of AGNs into primary continua and secondary components

H. Noda[1], K. Makishima[1,2,3], K. Nakazawa[1], and S. Yamada[2]

[1] Department of Astronomy School of Science, The University of Tokyo, 7-3-1, Hongo, Bunkyo-ku, Tokyo 113-0033, Japan, e-mail: noda@juno.phys.s.u-tokyo.ac.jp
[2] Institute of Physical and Chemical Research (RIKEN), Wako, Saitama 351-0198, Japan
[3] Research Center for the Early Universe, The University of Tokyo, 7-3-1, Hongo, Bunkyo-ku, Tokyo 113-0033, Japan

Abstract. Through a model-independent technique utilizing count-count correlations between a reference energy band and others, the 3–45 keV signal of the bright type I Seyfert NGC 3516 observed by *Suzaku* was decomposed into a variable component and a stable one. The reference energy band was chosen to be 2–3 keV, where the relative variation was largest. The variable component was reproduced successfully by a weakly-absorbed power-law model with a photon index of ~ 1.64. The stable component, if assumed to vanish in the reference band, fully agrees with reflection by neutral materials, with a moderate iron abundance of 1.2 Solar. If, in contrast, the reference band is assumed to contain significant amount of constant signals ($> 20\%$ of the maximum that is allowed by the data), the broad-band *Suzaku* data indicate the presence of an additional non-varying component that has not been recognized previously.

Key words. galaxies: active – galaxies: individual: NGC 3516 – X-ray: galaxies

1. Introduction

X-ray spectra from Active Galactic Nuclei (AGNs) consist of primary continua, generated by inverse Compton scattering in coronae, and secondary components which appear when the primary emission is Compton-scattered or photo-absorbed by materials surrounding the central black hole (BH). However, spectral shapes of these components are similar, particularly in hard X-ray band, so that it has been notoriously difficult to separate them by spectral analysis alone. To overcome this spectral ambiguity, time-variability of each spectral component is important. Noda et al. (2011a) succeeded in identifying multiple continuum components in the bright Seyfert MCG–6-30-15 referring to their different variations.

In the present paper, we focus on a timing method utilizing Count-Count Correlation with Positive Offset (C3PO method). It enabled us to extract soft X-ray excess components in several AGNs, and to identify them with thermal Comptonization emissions independent of the variable primary continuum (Noda et al. 2011b, Noda et al. 2013). When applied to harder X-ray bands of AGNs, this method is

Send offprint requests to: H. Noda

expected to decompose broad-band X-ray signals into a variable primary emission generated near the BH, and a stable emission produced generally at large distances from the BH. The latter includes a reflection component and Fe-K emission lines from distant cold materials, such as an outer disk and the molecular torus.

The present study chooses the typical and bright type I Seyfert galaxy NGC 3516 at a redshift 0.0885, because it has large X-ray variation amplitudes which are suited to the C3PO method. We analyzed *Suzaku* archival data of this AGN, obtained from 2009 October 28 5:35(UT) to November 2nd 12:39 (UT).

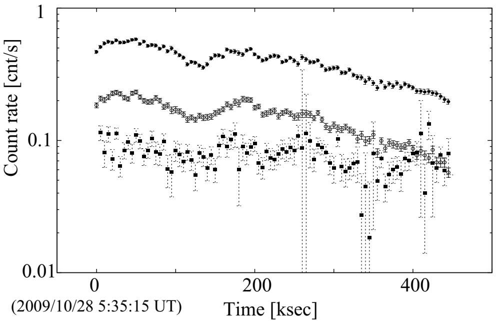

Fig. 1. Background-subtracted and dead-time corrected light curves of NGC 3516, obtained by XIS FI in the 2–3 keV (middle) and 3–10 keV (top) bands, together with the 15–45 keV HXD-PIN data (bottom), shown with a binning of 5 ksec. Error bars represent statistical 1σ ranges.

2. Model-independent separation of variable and stable spectra

2.1. Method of count-count correlation with positive offset

Figure 1 shows three-color light curves of NGC 3516 from the present *Suzaku* observation. While the 3–10 keV variation followed that in the 2–3 keV band, the 15–45 keV variation was milder at least on time scales of ~ 500 ksec. To study how intensities at different energy bands were correlated with one another, we employed the C3PO method (Noda et al. 2011b; Noda et al. 2013), and chose the 2–3 keV band as a reference because the RMS variability therein was relatively large at $\sim$35% in the present data, as well as in other observations of similar objects (e.g., Markowitz et al. 2003). Then, the remaining 3–45 keV broad band was divided into 16 finer bands with boundaries at 3.0, 3.5, 4.0, 4.5, 5.0, 5.5, 6.0, 6.25, 6.5, 6.75, 7.0, 7.5, 8.0, and 10.0 keV for the XIS, while at 15.0, 20.0, 30.0, and 45.0 keV for the HXD-PIN.

Then, we made 16 Count-Count Plots (CCPs), in which ordinate (denoted y) gives NXB-subtracted XIS FI or HXD-PIN count rates in the above bands, while abscissa (denoted x) is that in the 2–3 keV band used as the reference. Figure 2 shows three of them, where we find relatively tight correlations among different bands. The data in each CCP was fitted with one straight line, expressed by

$$y = Ax + B, \tag{1}$$

in which the slope A and the offset B are both left free. The fits were mostly acceptable, and gave positive offsets ($B > 0$). Thus, the variations in these energy bands can be explained by intensity changes of a single variable component with a fixed shape (represented by A), which is superposed on top of a separate constant spectral component (represented by B).

The C3PO method in its simplest form (e.g., Noda et al. 2011b) regards the assembly of A as a variable spectral component, and that of B as a stable one. However, this is based on an assumption that the reference band includes no stable emission. When this assumption is not warranted, we need to rewrite eq.(1) as

$$y = A(x - x_0) + B'; \quad B' \equiv B + Ax_0 \tag{2}$$

where x_0 is the ultimate intensity floor (or offset) in the reference band, to be attained when the variable-component intensity becomes zero. Since there is no *a priori* knowing of x_0, below we study five cases with $x_0 = 0$, $x_0 = 0.2x_0^{\mathrm{m}}$, c, and $x_0 = x_0^{\mathrm{m}}$, where x_0^{m} is the minimum intensity actually observed in the reference band (= highest intensity floor allowed by the data), ~ 0.05 cnts s^{-1} (Fig. 1).

2.2. The variable component

The variable spectrum can be constructed by multiplying the slope A of eq. (2) by $\bar{x} - x_0$,

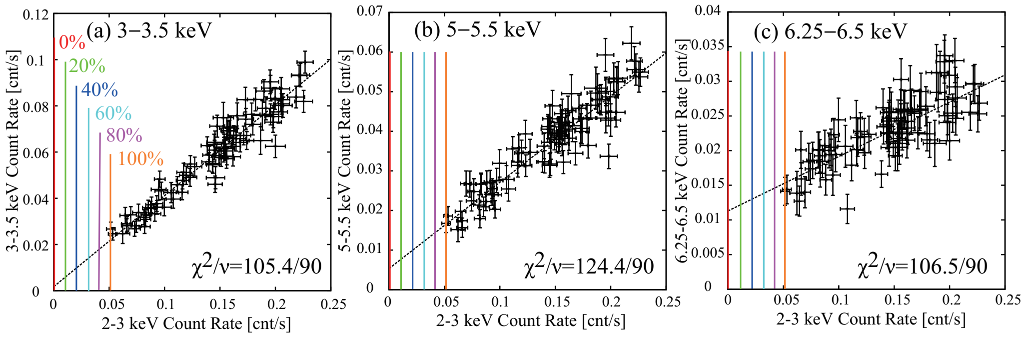

Fig. 2. Three CCPs representing the 16, in which abscissa gives NXB-subtracted XIS FI count rate in 2–3 keV, while ordinate that in the energy band indicated in each panel. All data are binned into 5 ksec, and the error bars represent statistical $\pm 1\sigma$ range. The straight line refers to equation (1). Colored lines shows 0% (red), 20% (green), 40% (blue), 60% (cyan), 80% (purple), and 100% (orange) levels of the maximal offset count rate of $x_0^{\mathrm{m}} \sim 0.05$ cnt s^{-1} that is allowed in the 2–3 keV band.

where $\bar{x} \sim 0.15$ cnt s^{-1} (Fig. 1) is the average intensity in the reference band, and dividing by the corresponding energy interval. The normalization of this component thus decreases as we adopt higher values of x_0 ($0 < x_0 < x_0^{\mathrm{m}}$), but its spectral shape remains the same. The results are plotted in Fig. 3(a) in νF_ν form.

The extracted variable component was successfully reproduced by an absorbed PL model, `wabs*cutoffpl`, where the column density and the photon index were obtained as $0.4^{+0.8}_{-0.4} \times 10^{22}$ cm^{-2} and $1.64^{+0.15}_{-0.11}$, respectively. As argued above, the choice of x_0 affects only the PL normalization. As ensured by the good linearity of the CCPs, this spectral component is considered to have varied in intensity only, without any slope change.

2.3. The stable component

When the values of B' in eq. (2) are divided by the corresponding energy intervals, we obtain the stable spectral component. As shown in Fig. 3(b), this component is sensitive, both in intensity and shape, to the choice of x_0; the higher it is assumed, the softer and brighter the stable spectrum becomes, because the Ax_0 term in the definition of B' is essentially the variable spectrum. In any case, the extracted component bears an intense Fe-K line at 6.33 keV (6.40 keV in the rest frame). Mathematically, the variable and the stable components sum up to become the time-averaged spectrum in any case.

If we assume $x_0 = 0$, the obtained stable spectrum is the hardest and similar to a reflection component generated by semi-finite material (such as an accretion disk) without strong ionization. Actually, this spectrum was reproduced successfully by an absorbed neutral-disk reflection model, `wabs*pexmon` in XSPEC12, with the iron abundance of $1.2^{+0.4}_{-0.3}$ Solar. Here, the photon index of the primary emission and the column density of the absorption were fixed at the same values as the variable component, 1.64 and 0.4×10^{22} cm^{-2}, respectively, and the cutoff energy and the inclination are at 150 keV and 30°, respectively. Thus, the stable component in this case can be interpreted as a pure neutral-disk reflection with a moderate iron abundance.

If, in contrast, x_0 is made higher than $\sim 0.2x_0^{\mathrm{m}}$, the stable component can no longer be explained by the neutral-disk reflection only, mainly due to positive residuals in the 3–6 keV band. To improve the fit, we need to include an additional spectral component, which is softer than the neutral-disk reflection model but possibly as hard as the average spectrum.

Let us represent the above additional component by an empirical absorbed PL model, `wabs*cutoffpl`, that is independent of the variable PL. We fitted the stable component with `wabs*(pexmon + wabs*cutoffpl)`,

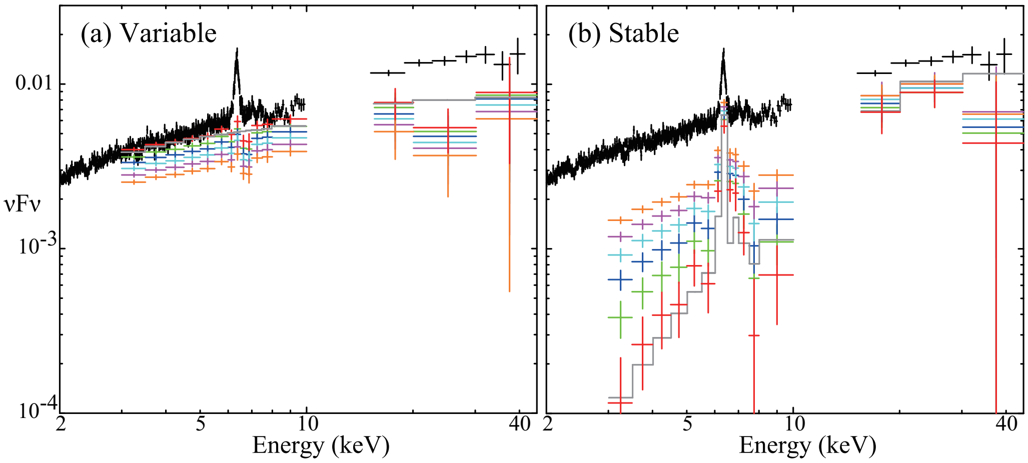

Fig. 3. Variable (panel a) and stable (panel b) spectra in νF_ν form, obtained by dividing A and B' of eq. (2) by the corresponding energy intervals, respectively. Red, green, blue, cyan, purple, and orange points represent $x_0 = 0, 0.2x_0^{\mathrm{m}}, 0.4x_0^{\mathrm{m}}, 0.6x_0^{\mathrm{m}}, 0.8x_0^{\mathrm{m}}$, and $x_0 = x_0^{\mathrm{m}}$, respectively, while black commonly represents the time-averaged spectrum. Grey line in (a) shows an absorbed PL model with a photon index of 1.64, and that in (b) a model of a neutral-disk reflection of which the photon index of the primary continuum, the cutoff energy, the iron abundance, and the inclination are 1.7, 150 keV, 1.2 Solar, and 30°, respectively.

where the column density in the second `wabs` and the photon index in the second `cutoffpl` were left free, while the other parameters were fixed like the previous fits. As a result, the fits became all successful with the column density of 0.8–6.0×10^{22} cm^{-2} and the photon index of 1.60–2.38 in any intensity floor except for the case of $x_0 = 0$. Furthermore, the sum of the models for the variable and stable components, `wabs*(cutoffpl + pexmon + wabs*cutoffpl)`, successfully reproduced the 2–45 keV time-averaged spectrum of NGC 3516, and gave the parameters which all are consistent with the individual fits to the variable and stable components. Thus, the additional spectrum to explain the stable component was revealed to have a shape consistent with that of an absorbed PL model.

3. Discussion and conclusions

The C3PO method developed in Noda et al. (2011b, 2013) successfully decomposed the 3–45 keV *Suzaku* spectrum of NGC 3516 into a variable and a stable components model-independently. To explain the obtained stable component, an absorbed-PL like model is necessary besides a neutral-disk refection, at any intensity floor except for $x_0 = 0$. This additional signal might be regarded as identical to the concept of partially-absorbed primary continuum. However, this interpretation, at least in its simplest form, is not supported by the data, since this additional component was stable over the present observation which lasted for 500 ksec. The additional component cannot be considered as a non-varying part of the variable component, either, since the fit to the stable component failed, regardless of x_0, when the photon index and the total absorption were fixed at those of the varying component. Possible interpretations of this new component will be discussed elsewhere.

References

Markowitz, A., Edelson, R., & Vaughan, S. 2003, ApJ, 382, 194
Noda, H., et al. 2011a, PASJ, 63, 449
Noda, H., et al. 2011b, PASJ, 63, S925
Noda, H., et al. 2013, PASJ, in press, `arXiv:1208.3536`